Journal of Archaeological Science 40 (2013) 778–785

Contents lists available at SciVerse ScienceDirect

Journal of Archaeological Science

journal homepage: http://www.elsevier.com/locate/jas

Is X-ray diffraction able to distinguish between animal and human bones?

Giampaolo Piga [a,b,*], Giuliana Solinas [c], T.J.U. Thompson [d], Antonio Brunetti [e], Assumpció Malgosa [a], Stefano Enzo [b]

[a] GROB (Grup de Recerca en OsteoBiografia), Unitat d'Antropologia Biologica, Department de Biologia Animal, Biologia Vegetal i Ecologia, Universitat Autonoma de Barcelona, Edifici C, 08193 Bellaterra, Barcelona, Spain
[b] Dipartimento di Chimica e Farmacia, Università di Sassari, via Vienna 2, I-07100 Sassari, Italy
[c] Department of Biomedical Sciences, Laboratory of Epidemiology and Biostatistics, University of Sassari, via Padre Manzella 4, I-07100 Sassari, Italy
[d] School of Science & Engineering, Teesside University, Borough Road, Middlesbrough TS1 3BA, UK
[e] Struttura Dipartimentale di Matematica e Fisica, Università di Sassari, via Vienna n. 2, I-07100 Sassari, Italy

Keywords:
Powder X-ray diffraction
Heat treatment
Hydroxylapatite
Lattice parameters
Human bones
Animal bones
Human bone identification

A B S T R A C T

The possibility of determining the human or animal origin of bones from the lattice parameters of their inorganic bioapatite phase, when subjected to a high temperature treatment using the powder X-ray diffraction (XRD) technique, has been explored on a wide number of specimens. Forty-two animal bones were treated in a furnace at 1100 °C for 36 min and compared to 53 cremated human bones from a range of ancient necropolises. The X-ray diffraction patterns of bioapatite were simulated using both monoclinic P21/b and hexagonal P63/m structures to verify any occurrence of phase transformation and any difference in the lattice parameters due to the model. It was determined that the differences between the *a*-axis and *c*-axis of the monoclinic and hexagonal lattice were unimportant. Some outlying values were revealed to be caused by the presence of chlorine ions diffused into the apatite structure increasing its average unit cell values. Nevertheless, our results clearly show that in terms of lattice parameters the variability of human specimens are completely overlapped by the non-human variability making the use of XRD in order to distinguish animal from human bones questionable.

1. Introduction

The separation of animal from human bone is an important component of any archaeological or forensic osteological and histological analysis (Cattaneo et al., 1999; Cuijpers, 2006; McKinley, 1994; Whyte, 2001). It can be important for a range of reasons, from determining the minimum number of individuals present, to understanding funerary behavior, to comprehending human–faunal relations. This is also true of burned skeletal material, but this work is greatly complicated by the range of heat-induced changes that bone undergoes when burned (Thompson, 2005). Thus studies which focus on the separation of different species of bone, especially if fragmented, are extremely valuable. With this in mind, Beckett et al. (2011) reported in a recent paper the possibility of determining the human rather than animal origin of bone from the lattice parameters of the inorganic bioapatite phase from the diffraction patterns of bones subjected to a high temperature heating treatment. Actually, the structural properties of a substance are inspected by diffraction in terms of symmetry operations compatible with three-dimensional periodicity of the crystals, i.e., specifying one of the 230 possible space groups (see: International Tables for X-ray Crystallography, 1965–68), complemented with the geometry and dimensions of the unit cell of the lattice (so-called lattice parameters) as well as its atomic content and arrangement. For the case of bioapatite crystals found in bones, a space group $P6_3/m$ is generally attributed with a hexagonal unit cell where two lattice parameters *a*- and *c*-axis respectively, need to be determined. According to Beckett et al. (2011), the plot of *a*- vs *c*-axis data points from human being occurs in a typical and distinct area with respect to animals.

The determination of lattice parameters depends upon the precision of locating the peak profiles in XRD diagrams (Masciocchi and Artioli, 1996), but in bioapatite this is difficult to do. This is because of large peak broadening resulting from the small crystallite size of the phase combined with the high amount of lattice strain (Danilchenko et al., 2002). To alleviate this problem, Beckett et al. (2011) have suggested that lattice parameter determination be performed on highly crystallized single phase materials following

* Corresponding author. GROB (Grup de Recerca en OsteoBiografia). Unitat d'Antropologia Biologica, Department de Biologia Animal, Biologia Vegetal i Ecologia, Universitat Autonoma de Barcelona, Edifici C, 08193 Bellaterra, Barcelona, Spain.
E-mail address: kemiomara@yahoo.it (G. Piga).

0305-4403/$ – see front matter © 2012 Elsevier Ltd. All rights reserved.
http://dx.doi.org/10.1016/j.jas.2012.07.004

thermal treatment of the bone. However this in turn creates a potential problem in identifying the most appropriate heating temperature for differentiating faunal from human bone.

Another potential issue with the approach in Beckett et al. (2011) stems from the fact that their analysis is limited to a sample of just 8 human specimens vs 65 non-human samples from 12 different species. This may be due to the difficulties in acquiring modern bone for such research, but nevertheless the large availability of human bones from the archaeological context offers considerable scope for the continued investigation of this area (Piga et al., 2007). Thus we have critically investigated the diffraction patterns of a wide variety of bones originating from various contexts routinely met in the course of our archaeological and anthropological investigations (Piga et al., 2010a, 2010b).

Unfortunately the factors regulating the chemistry of bones are still not completely known. Apatites have the general formula, $Ca_5(PO_4)_3X$ or $Ca_{10}(PO_4)_6X_2$ where X is typically F (fluorapatite), OH (hydroxylapatite), or Cl (chlorapatite) in case of natural minerals (Elliott et al., 2002). Typically the mineral of bone and teeth is an impure form of OHA where the major variations in composition focus on a variable Ca/P mol ratio (1.6–1.7, OHAp is 1.66), and a few percent CO_3^{2-} and water. In fact, the apatite lattice is very tolerant to substitutions, vacancies and solid solutions; for example, X in the general chemical formula above can be replaced by $½CO_3^{2-}$ or $½O^{2-}$; Ca^{2+} by Sr^{2+}, Ba^{2+}, Pb^{2+}, Na^{+} or vacancies; and PO_4^{3-} by HPO_4^{2-}, AsO_4^{3-}, VO_4^{3-}, SiO_4^{4-} or CO_3^{2-}. It is the degree of such substitutions that can affect the average lattice parameter values and introduce some voids or strain (Aellach et al., 2010), and these may also be responsible for the unique mechanical properties of bone. Other factors affecting the lattice parameter are the presence of organic materials of biogenic origin, and extra phases (Elliot, 1994).

Wopenka and Pasteris (2005) have recently discussed the oversimplifications involved when using the hydroxylapatite inorganic phase as a model of bones, especially in view of the types of ionic substitutions that can occur in the apatite lattice which may then change the mineral characteristics of the bone material. Instead, Wopenka and Pasteris (2005) locate natural bioapatite inside a hyper-phase diagram with end-members of apatite minerals such as hydroxylapatite, fluorapatite, A-type carbonated apatite, B-type carbonated fluorapatite (formerly known as francolite), and B-type carbonated hydroxylapatite (formerly known as dahllite).

Of course, *post-mortem* taphonomic and diagenetic changes are expected to add further complexity to the structure and microstructure of bones, not only due to new ionic substitutions but also in terms of new biogenic or authigenic phases that form during the conservation, storage and degradation processes of bone (Shinomiya et al., 1998; Piga et al., 2009a, 2011).

The paper by Beckett et al. (2011) has employed a simplified approach for lattice parameter determination starting from the peak positions which are calculated by the automatic location of the maxima of diffraction patterns (which may not be completely satisfactory). In our work care has been exercised in order to measure the lattice parameters of the bioapatite phase with the best practices ensuring precision and accuracy. The Rietveld method (Rietveld, 1967; Young, 1993) appears to be the most orthodox approach for this purpose (Peterson, 2005) and indeed is now standard practice in materials science (although its use has appeared only sporadically in the archaeological and forensic fields). Another important point concerns the most suitable space group for describing the bioapatite structure when using powder XRD. While the most popular space group to represent the structure of bioapatite is $P6_3/m$, a more suitable alternative appears to be a monoclinic description using the $P2_1/b$ space group. This is due to the fact that OH− is non-spherical and therefore reduces possible crystalline symmetry (Elliott et al., 1973; Wopenka and Pasteris, 2005). Moreover, we must also bear in mind that it was recently reported that a monoclinic-to-hexagonal order/disorder transformation occurs at 220 °C for synthetic apatite (Yashima et al., 2011).

In this work, first we address the problem of whether the monoclinic $P2_1/b$ vs hexagonal $P6_3/m$ space group can make a substantial difference in terms of lattice parameter values for the bioapatite of bones. We then evaluate the most evident structural changes involved after high-temperature treatment. Finally we discuss the lattice parameter values of heat-treated animal and human bone samples from various Spanish and Italian necropolises.

2. Experimental methodology

2.1. Examined specimens

The forty-two animal bone specimens were kindly made available from: the Institut Català de Paleontologia (Sabadell-Barcelona, Spain), the School of Science & Engineering, Teesside University (UK), and the Department of Animal Biology, University of Sassari (Italy). Our collection consists of 25 species, distributed as it follows: mammoth (3), monkey (3), camel (1), deer (2), rhino (1), horse (2), ox (1), pig (1), ruminant (2), sheep (1), goat (2), rodent (1), lagomorph (2), cat (1), lion (1), dog (1), fox (1), crocodile (1), turtle (2), bird (6), whale (1), dolphin (3), tuna (1), swordfish (1), shark (1). The specimens date from the present time back to 900,000 years ago.

Further, the fifty-three human bones were kindly made available from: the Universitat Autonoma de Barcelona (Spain), and the Department of History, University of Sassari (Italy). These bones originate from: the Necropolis of *Aguilar de Montuenga* (Soria, Spain), the Necropolis of *Son Real* and *S'Illot des Porros* (Mallorca, Spain) (Piga et al., 2010b), the Necropolis of Sebès (Tarragona, Spain) (Belarte and Noguera, 2008), the Necropolis of *Mas d'en Boixos* (Pacs del Penedès, Alt Penedès, Spain) and the Necropolis of *Monte Sirai* (Carbonia, Italy) (Guirguis, 2010). Synthetic powder hydroxylapatite was synthesized by Aldrich Chemistry®.

2.2. Thermal treatment

In the present study we have selected historical human bones burned at temperatures above 1000 °C. This is based on our previous laboratory calibrations (Piga et al., 2008, 2009b). The animal bones were subjected to a heat treatment at 1100 °C for 36 min in a furnace, in order to sharpen the peak profiles to be used for determination of the lattice parameters.

2.3. Diffraction data collection and analysis

Exactly 0.5 g of each bone was ground in an agate jar for 1-min using a SPEX mixer-mill model 8000. Our sample holder for XRD analysis has a circular cavity of 25 mm in diameter and 3 mm in depth, and can hold 420 mg of pressed powder bone.

The Bruker D8 instrument was employed in the Bragg-Brentano geometry using fixed wavelength CuKα radiation and a graphite monochromator in the diffracted beam. The patterns were collected with a scintillation detector in the 2θ angular range from 9 to 140°, with a step-size of 0.05°; the counts at each data point being accumulated for 40 s in order to ensure accurate statistics for the intensity data and to reduce the uncertainty associated with the determination of lattice parameters. The X-ray generator worked at a power of 40 kV and 40 mA and the resolution of the instruments (0.5° divergent and 0.1 mm antiscatter slits) was determined using

α-SiO_2 and α-Al_2O_3 standards which were free from the effect of reduced crystallite size and lattice defects (Enzo et al., 1988).

The precision and accuracy of lattice parameters depends largely upon the number of peaks assessed and the relative location in the 2θ scale with respect to the whole angular range investigated (Masciocchi and Artioli, 1996; Peterson, 2005). Note that the use of position sensitive detectors for faster data collection may speed-up the data collection, the configuration used here (with a monochromator in the diffracted beam) has the advantage of controlling the background due to specific fluorescence effects. This will increase the time taken for data collection, and we are aware that the laboratory high-resolution conditions may be overtaken by accessing synchrotron radiation facilities for powder XRD.

The Rietveld method (Rietveld, 1967; Young, 1993) is based on an iterative best-fit strategy of experimental data. We have made use of the MAUD programme (for: *Material Analysis Using Diffraction*) which simulates the pattern by incorporating the instrument function and convolving the crystallographic model based on the knowledge of chemical composition and space group with selected texture and microstructure models (Lutterotti and Bortolotti, 2003). The programme permits a selection of variables for the least squares minimization such as lattice parameters of the unit cell, atomic positions, temperature factors, occupancy of the sites, an/isotropic size and strain broadening. In all patterns we have verified whether the monoclinic $P2_1/b$ rather than hexagonal $P6_3/m$ choice of the space group may have direct consequences for the analyzed values of the lattice parameters. The success of the procedure is generally evaluated throughout a combination of integrated agreement factors (R_{wp} is the most considered) and distribution of residuals (Young, 1993).

2.4. XRF analysis

XRF measurements have been carried out using portable equipment composed of an X-ray tube (molybdenum anode, Oxford Instruments) working at 25 kV and 0.1 mA. For the analysis we pressed ~200 mg of powdered bone tissue to form a pellet with a diameter of 10 mm and a thickness of 1 mm. An aluminum collimator 1 cm long and with an internal hole of 1 mm in diameter permits irradiation of an area of the object of about 0.2 cm^2 to be analyzed, at a distance tube window-sample of about 2 cm. A Si-PIN detector from AMPTEK was employed with a thickness of about 300 μm and characterized by an energy resolution of about 200 eV at 5.9 keV. 30 min was dedicated for each sample pattern without use of any standard.

2.5. Statistical analysis

All statistical analysis was performed using Stata software 9.0. In order to investigate the relationship between *c*-axis and *a*-axis values of the monoclinic (pseudo hexagonal) phase we have used the regression analysis by assuming the *a*-axis as the independent variable. Moreover, the Grubbs test was applied with 95% confidence to detect outliers (Grubbs, 1950).

3. Results and discussion

The diffraction patterns of the bones, prior to any thermal treatment conformed to the general appearance of a succession of peaks, attributable to the apatite lattice. Almost all specimens examined here showed a single-phase character, making the XRD structure analysis relatively simple. The widely broadened succession of profiles (see Fig. 1) is generally interpreted in terms of fineness of the apatite average crystallite size and short range disorder in the lattice. In fact the scatter due to collagen and organic components – if present – is negligible and would not affect our data interpretation.

In unburned bioapatites, the XRD line broadening of the (001) peak narrower than the other profile indices (whether in hexagonal or monoclinic description) may be taken as an indication of the anisotropic shape of the crystallites. This behavior is accounted for by the MAUD program with the Popa model (Popa, 1998). In general the model fit results suggest very small average crystallite size whose shape is elongated along the *c*-axis, as it is displayed in the Fig. 1B.

The longer "characteristic size" varies from 80 to 160 Å in unburned bones, which is in agreement with direct observation by Transmission Electron Microscopy and previous XRD work conducted on human fetal bones (Meneghini et al., 2003). Of course various definitions of the average size length can be envisaged when working with particles with irregular shape (Matyi et al., 1987). Note that the behavior of the bioapatite in terms of smallness of crystallite size and strain is different from synthetic hydroxylapatite, where such small characteristic dimensions cannot be achieved. For example, in Fig. 1C we see that the synthetic OHAp, which is supposed to be very pure from the chemical point of view, displays a single-phase condition with relatively sharp peaks in the as-prepared material.

The lattice parameter values *a*- and *c*-axis respectively in the two unburned specimens are reported in Table 1 and appear significantly different even when using a monoclinic space group. This may be related to the diffuse profiles of the pattern. Some shape anisotropy seems to be confirmed by the Popa model as reported in the Fig. 1D (Popa, 1998).

3.1. Transformation behavior of natural and synthetic apatites thermally treated up to 1100 °C

On sintering the bioapatite with thermal treatment, the degree of anisotropic broadening is partially removed from the patterns due to the coarsening mechanism attributable to the temperature treatment. This must be of the coalescence type (Granqvist and Buhrman, 1977). The diffraction data of ox burned bone (Fig. 2A) show narrow peaks and the quality of the fit appears "satisfactory" on the basis of the percentages from the agreement factors (see the R_{wp} values reported in the Table 1). Some anisotropy is still present since the average crystallite size depicted by the anisotropic model has a "potato"-like shape (as shown in the Fig. 2B). Of course we should keep in mind that for this and many other heat-treated specimens, the average size length is ca 1600 Å, i.e., around values close to the instrument resolution limit, above which no larger average crystallites can be assessed by the applied instrumentation (Piga et al., 2008, 2009b).

In a comparison of the monoclinic vs hexagonal geometry we see in Table 1 that the agreement numerical factors for the monoclinic phase are performing slightly better than the hexagonal description in fitting the same experimental data. This further suggests the opportunity for using the monoclinic structure to describe the bioapatite structure, even for high-temperature specimens. The monoclinic space group appears to produce an average crystallite size value slightly larger than when using the hexagonal description for the unburned bones.

It should be recognized that the monoclinic space group deals not only with four lattice parameters adjustable for the best fit but also with a total of 67 parameters due to the atomic coordinates of 5 Calcium, 3 Phosphorous, 12 Oxygen and one OH^-. This is definitely larger than for the hexagonal phase where the procedure adjusts only two lattice parameters and 12 atomic coordinates (Posner et al., 1958). Moreover, even the modeling of microstructure

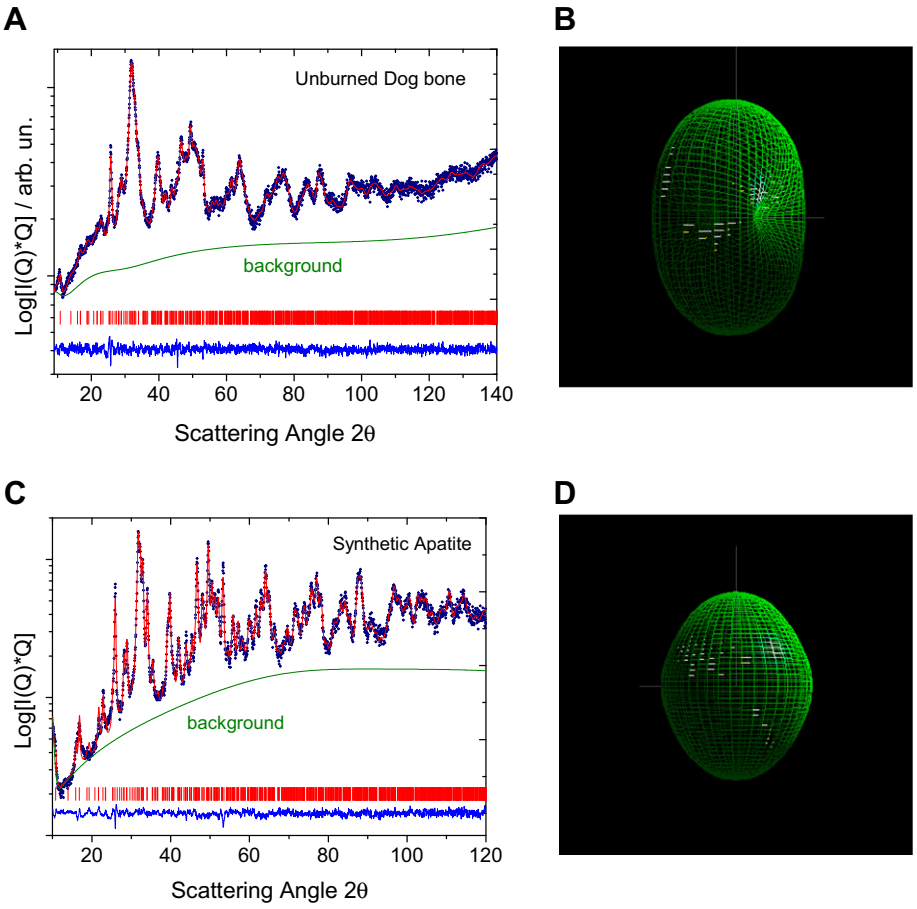

Fig. 1. A) Experimental pattern (data points) and Rietveld fit (full line) of a typical bioapatite from unburned dog bone. The agreement between experiment and model appears satisfactory as it can be concluded from the inspection of residuals (see band at the bottom) and after evaluation of the agreement factor R_{wp}. Nevertheless the procedure has unavoidably an uncertainty associated to the precise location of the peak profiles due to their large broadening. This affects the reliability of the lattice parameter values. B) The figure depicts the average shape of apatite crystallites elongated along the *c*-axis, which is reconstructed from the difference among hkl peak broadening. C) Experimental pattern (data points) and Rietveld fit (full line) of an apatite synthesized in the laboratory according to the equation: $5Ca(OH)_2 + 3H_3PO_4 > Ca_5(PO_4)_3OH + 8H_2O$. The full XRD pattern appears sharper than in the previous case testifying the difficulties in science to mimic a physiological reaction even though the average anisotropic shape (1D) is similar (not the size).

parameters according to Popa (1998) involves a larger number of anisotropic terms in the monoclinic vs hexagonal description. Accounting properly for these detailed parameters may constitute a serious limitation of the monoclinic description in view of the appeal of modeling the whole range of physico-chemical information of the bone with a simpler structure.

One further interpretation related to the chemical composition of bone may be revealed in the single-phase character of the examined samples. We are used to thinking of the inorganic "apatite" component as a single phase after the water and organics are removed, but this may not always be the case once the bone is subjected to a high-temperature treatment. In fact we have verified

Table 1
Comparison of lattice parameter, average crystallite size and agreement factor values for the couple of unburned and heat-treated specimens of dog bone and synthetic apatite, respectively.

Specimen	Hexagonal $P6_3/m$ cell				Monoclinic $P2_1/b$ cell					
	a-axis/Å	*c*-axis/Å	<D>/Å (±10%)	Rwp/%	*a*-axis/Å	*b*-axis/Å	*c*-axis/Å	γ-axis/°	<D>/Å (±10%)	Rwp/%
Synthetic apatite	9.448 (±0.003)	6.880 (±0.001)	286	9.9	9.457 (±0.003)	18.906 (±0.005)	6.884	120.08 (±0.05)	320	7.6
Heat treated synthetic apatite/whitlockite	9.427 (±0.001)	6.8830 (±0.0004)	1070	7.4	9.422 (±0.001)	18.846 (±0.002)	6.882 (±0.0004)	119.93 (±0.05)	1070	6.7
	10.438 (±0.002)	37.438 (±0.005)	1630		10.438 (±0.002)		37.434 (±0.005)		1650	
Unburned Dog bone	9.443 (±0.005)	6.905 (±0.002)	110	5.80	9.432 (±0.005)	18.865 (±0.01)	6.9047 (±0.0005)	119.90 (±0.05)	120	4.2
Burned Dog bone	9.423 (±0.001)	6.8840 (±0.0005)	1430	13.2	9.421 (±0.001)	18.849 (±0.002)	6.8841 (±0.0005)	120.00 (±0.05)	1640	11.2

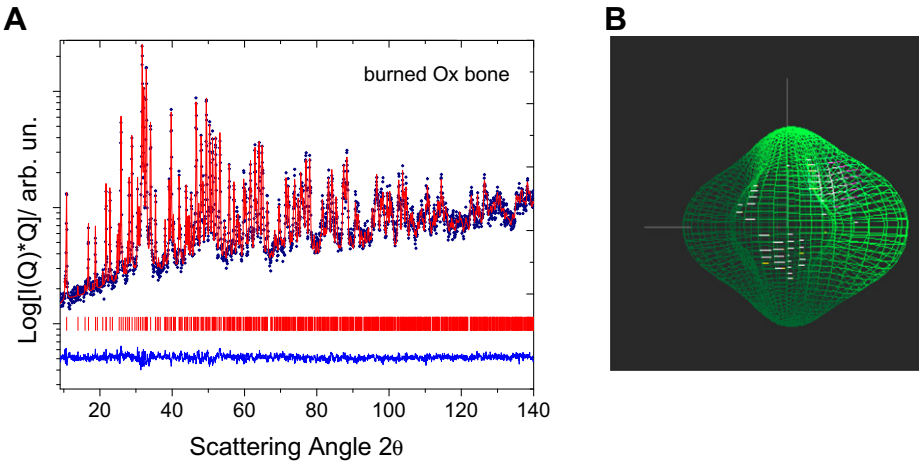

Fig. 2. A) Pattern of a burned ox bone and B) its Rietveld fit using a monoclinic space group for apatite. The approximate, average crystallite shape from Popa model is also reported on account of the observed anisotropic line broadening.

that for biological carbonate apatites treated above 850 °C, the removal of carbonate groups results in the formation of CaO after cooling down to room temperature (RT). When the synthetic powder is subjected to a thermal treatment at 1100 °C for 36 min, not only we notice peak sharpening (useful to determine accurately lattice parameters) but find also a multi-phase condition for the resultant product (see Fig. 3A). This is due to a well-known transformation of a part of OHAp to whitlockite, i.e., to the β-three-calcium-phosphate phase with chemical formula $Ca_3(PO_4)_2$ according to the reaction equation:

$$Ca_{10}(PO_4)_6(OH)_2\,(HT-1100\,^{\circ}C) \rightarrow 3\,\beta-Ca_3(PO_4)_2 + CaO + H_2O$$

Conversely, the bone specimens that have been treated thermally at 1100 °C (in order to make the determination of the lattice parameter values clearer), did not display the important phenomena of phase separation and precipitation apart from two specimens of cormorant (15% and 9% wt of whitlockite, respectively) and a pig bone (see Fig. 3C, bottom pattern). For the pig bone we notice that the unburned bioapatite is less "crystalline" than the synthetic apatite but also that the amount of β-$Ca_3(PO_4)_2$ is definitely lower (23% wt) than in the previous case. In both cases even the average shape of whitlockite was revealed to be isotropic (Fig. 3B and D). Thus we can infer that the mechanical and thermodynamic properties of bone are influenced by the type and nature of atomic substitutions occurring in the apatite lattice. Note that we report the lattice parameters for the apatite phase that have been worked out for human and animal specimens using both the monoclinic $P2_1/b$ and hexagonal $P6_3/m$ unit cells in the Supplementary Tables.

The merit of using the monoclinic cell for describing the apatite structure is that the agreement factors of R_{wp} are systematically lower with respect to the hexagonal description. In general both hexagonal and monoclinic descriptions carried out on the same specimen give reasonably similar lattice parameters values but a higher variability of the results is encountered with the monoclinic case for the untreated specimens. Because the β angle parameter of the monoclinic structure remains close to 120°, the main variability is associated with the *b* lattice parameter (which may deviate significantly from twice the *a* parameter). Whether parameter *b* carries a precise physical meaning or not is difficult to establish in the presence of such very broad peaks. In fact, the standard deviation estimated from the untreated natural bones are relatively large and may be the effect of the large peak broadening, invariably related to a strong parameter correlation due to the mathematical difficulties in fitting the experimental data. In any case the *a-axis* and *c-axis* lattice parameters of the heat treated bones turn out to be the same (within the experimental uncertainty) in both the hexagonal and monoclinic representation.

It may be safe to conclude that, although the monoclinic description of bioapatites found by Elliott et al. (1973) appear to be more suitable for the problem in hand, using the hexagonal approach does not involve significant departures when accounting for the biological lattice of bones.

With these assumptions in mind, plotting animal and human bones lattice parameters in a *a*-axis vs *c*-axis plot as done in Fig. 4 permits verification or rejection of the differences between human bones with respect to non-humans. The ellipses drawn are showing the 95% degree of confidence for each group. The size of the ellipse is strongly influenced by the size of the dataset: the larger the number of data, the tighter the ellipse, even though the spread of data may be large.

From Fig. 4 we can clearly see just one outlier for humans while for non-human the outliers are distributed at shorter and larger values along the *c*-axis. This behavior suggests the presence of at least one more variable affecting the non-humans data. Nevertheless, in Fig. 4 we can see that the distribution of data points for non-human bone overlays the scatter for human bones, contrary to the previous findings (Beckett et al., 2011), therefore suggesting we reject the possibility of using XRD to distinguish human vs animal bones.

The transverse behavior for the ellipse of non-humans can be explained by a physical effect presumably occurring *post-mortem* for some specimens. In particular, the specimens that show shorter *a*-axis values were likely subjected to fluorination reaction, as they refer to paleontological bones (Piga et al., 2009a, 2011).

For the specimens with unusually large *a*-axis lattice parameters, which are exclusively modern bones, we can conjecture that the processing of cleaning the bones involving boiling in salted water has led to partial chlorination with consequent cell expansion mainly in the *a*- (and *b*-) direction. This is confirmed by examining the published lattice parameter values of Chlorapatite (Mackie et al., 1972). Indeed recent work has already demonstrated the effect of chlorine ions on bone when heated in salt water (Trujillo-Mederos et al., 2011) even if no correlation has been established with the lattice parameter values. Note also that the process of boiling the bones in salted water is not a cleaning practice common to archeology and forensics field. Increase of the

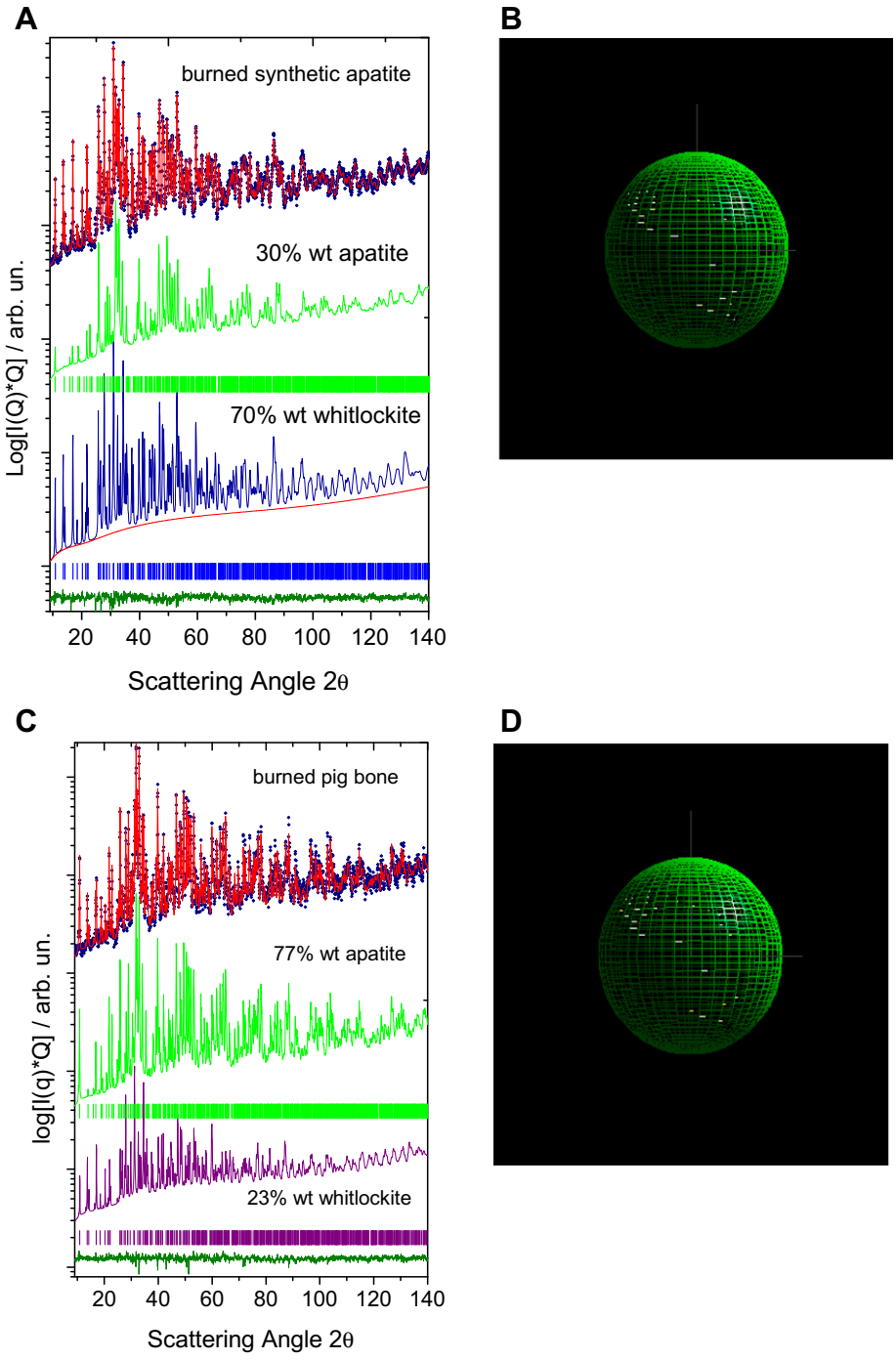

Fig. 3. A) The top of the figure depicts the XRD pattern and its Rietveld fit for the synthetic apatite thermally treated at 1100 °C, which turns out to be a mixture of 70 wt% of whitlockite and only 30% of monoclinic apatite. B) The broadening analysis revealed an isotropic average crystallite size of the apatite component of ca 1000 Å. C) For comparison the bottom pattern refers to the results from the pig bone burned at 1100 °C, one of the rare biological specimens showing a partial transformation to whitlockite. The amount of bioapatite is ca 77 wt% i.e., only 23 wt% belongs to whitlockite on account of a better stability of the biological vs synthetic phase synthesized at RT. D) Note again an isotropic shape of for the average crystallite size of ca 1700 Å for the bioapatite, close to the resolution limit of the instrument. In both cases even the average shape of whitlockite was revealed to be isotropic.

a- and *c*-axis parameter as a function of chlorine concentration were reported recently on synthetic hydroxy-chlorapatites solid solutions by Kannan et al. (2006).

As a matter of fact, the XRF spectra of these specimens in Fig. 5 indeed show the presence of Chlorine, which is readily exchanged in the bone matrix due to the unit cell dimensions of apatite. Of course other anions and cations may be responsible for an observed lattice parameter increase. Moreover, in particular cases the effect of expansion to the cell brought about by the chlorine anions may be compensated by the presence of other small ions. It can be argued that "routine" protocols adopted for cleaning prior to classification of bones may need some further calibration in view of their consequences on bioapatite chemistry and lattice parameter values.

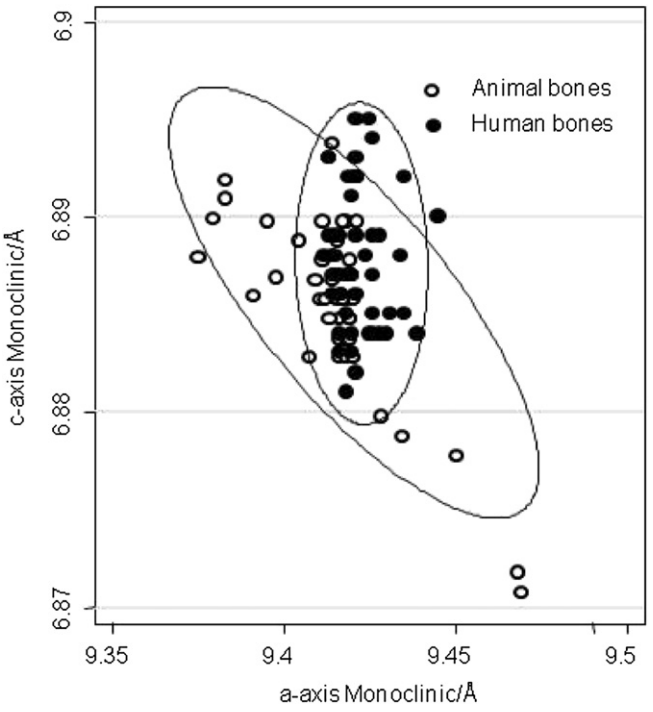

Fig. 4. Plot of *c*- vs *a*-axis for the two groups of bones treated at high-temperature (either in the furnace or after a crematory ritual). Apart from some outliers related to their fossilization processes or to inclusions of chlorine, the two groups of humans and animal bones are overlapped so as to identify a single cluster.

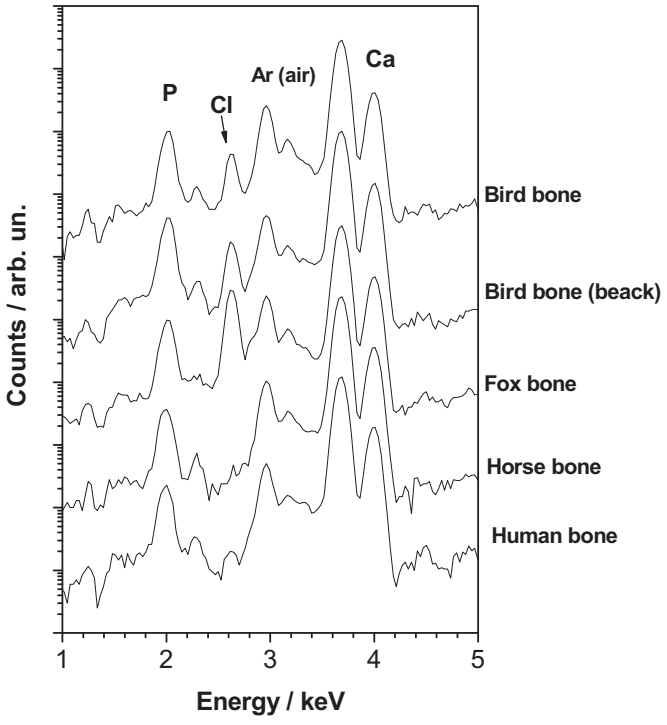

Fig. 5. The XRF spectra of three outlyiers (bird, bird beak and fox bone) compared to the spectrum of human and horse bones that did not show significant departure of its lattice parameters from the calculated average. This suggests that the presence of specific impurities in the bone lattice is relatable to the observed changes in lattice parameters. It is questionable to relate it just to the animal rather then human species.

4. Conclusions

The large availability of burned human bones from some ancient Spanish and Italian necropolises has been exploited in order to assess whether the lattice parameters of bioapatite obtained by XRD are helpful when trying to distinguish human bones from those of animals.

The lattice parameters of bioapatite were measured using the Rietveld method with a relatively high degree of precision on bones subjected to a high-temperature treatment. The bones were heated since this produces a readily observable sharpening of peaks resulting from the growth of the crystallites. While the synthetic apatite was partially transformed to whitlockite after 36 min at 1100 °C, the human bones were unaffected by this transformation. Moreover, this transformation partially occurred in just three of the animal bones studied. It is also useful to note that the *a*-axis and *c*-axis values of bioapatite are not biased by the use of a $P2_1/b$ monoclinic rather than $P6_3/m$ hexagonal unit cell. The different diet of the human species does not appear to affect the chemical composition of bones to the point of inducing systematic differences in the apatite lattice parameters, because of faults, inclusion of extra atoms and/or solid solution formations. However, the apatite unit cell axis can be affected by ion exchange reactions occurring *post-mortem* such fluorination during diagenesis or chlorination during boiling the bones in salted water for cleaning.

On the basis of our experiments involving 42 animal and 53 human bones it is not possible to discriminate human from non-human origin using lattice parameter values and any such claims to be able to do so should be treated with caution.

Our results are perhaps not so surprising, since the biological reactions that lead to the formation of apatite are conducted in a physiological environment that is chemically the same whether dealing with animals or humans.

Acknowledgments

The authors thank Prof. Salvador Moya Solà (Universitat Autonoma de Barcelona; Institut Català de Paleontologia), Angel Galobart, Jordi Galindo Torres, Laura Celià Gelabert (Institut Català de Paleontologia), Prof. Marco Zedda (Dipartimento di Biologia Animale, University of Sassari, Italy), Prof. Piero Bartoloni, Dr. Michele Guirguis, Alessandro Contini (University of Sassari, Italy) and Dr. Massimo Piccinini (Porto Conte Ricerche Science Center, Sassari, Italy); G. Piga is supported by the Regione Autonoma of Sardegna (Italy) within the project "Giovani Ricercatori" entitled: Studio archeometrico, antropologico e paleogenetico del materiale archeologico appartenente al sito fenicio-punico di Monte Sirai (Carbonia).

Appendix A. Supplementary data

Supplementary data related to this article can be found online at http://dx.doi.org/10.1016/j.jas.2012.07.004.

References

Aellach, B., Ezzamarty, A., Leglise, J., Lamonier, C., Lamonier, J.F., 2010. Calcium-deficient and stoichiometric hydroxyapatites promoted by cobalt for the catalytic removal of oxygenated volatile organic compounds. Catalysis Letters 135, 197–206.

Beckett, S., Rogers, K.D., Clement, J.D., 2011. Inter-species variation in bone mineral behavior upon heating. Journal of Forensic Sciences 56, 571–579.

Belarte, M.C., Noguera, J., 2008. El jaciments protohistòrics de Santa Madrona (Ribaroja) i Sebes (Flix), Ribera d'Ebre. Tribuna d'Arqueologia 2007, 127–147.

Cattaneo, C., Di Martino, S., Scali, S., Craig, O.E., Grandi, M., Sokol, R.J., 1999. Determining the human origin of fragments of burnt bone: a comparative study

of histological, immunological and DNA techniques. Forensic Science International 102, 181–191.
Cuijpers, A., 2006. Histological identification of bone fragments in archaeology: telling humans apart from horses and cattle. International Journal of Osteoarchaeology 16, 465–480.
Danilchenko, S.N., Kukharenko, O.G., Moseke, C., Protsenko, I.Yu., Sukhodub, L.F., Sulkio-Cleff, B., 2002. Determination of the bone mineral crystallite size and lattice strain from diffraction line broadening. Crystal Research and Technology 37 (11), 1234–1240.
Elliot, J.C., 1994. Structure and Chemistry of the Apatites and Other Calcium Orthophosphates. Elsevier, Amsterdam.
Elliott, J.C., Mackie, P.E., Young, R.A., 1973. Monoclinic hydroxyapatite. Science 180, 1055–1057.
Elliott, J.C., Wilson, R.M., Dowker, S.E.P., 2002. Apatite structures. Advances in X-ray Analysis 45, 172–181.
Enzo, S., Fagherazzi, G., Benedetti, A., Polizzi, S., 1988. A profile-fitting procedure for analysis of broadened X-ray diffraction peaks. I Methodology. Journal of Applied Crystallography 21, 536–542.
Granqvist, C.G., Buhrman, R.A., 1977. Size distributions for supported metal –catalysts – coalescence growth versus Ostwald ripening. Journal of Catalysis 42, 477.
Grubbs, F.E., 1950. Sample criteria for testing outlying observations. Annals of Mathematical Statistics 21, 27–58.
Guirguis, M., 2010. Necropoli fenicia e punica di Monte Sirai. Indagini archeologiche 2005–2007. In: Studi di Storia Antica e di Archeologia, vol. 7. Ortacesus ed., Cagliari.
International Union of Crystallography, 1965-68. International Tables for X-ray Crystallography. The Kynoch Press, Birmingham.
Kannan, S., Rocha, J.H.G., Ferreira, J.M.F., 2006. Synthesis of hydroxy-chlorapatites solid solutions. Materials Letters 60, 864–868.
Lutterotti, L., Bortolotti, M., 2003. Object oriented programming and fast computation techniques in MAUD, a program for powder diffraction analysis written in java. IUCr: Computing Commission Newsletter 1, 43–50.
Mackie, P.E., Elliott, J.C., Young, R.A., 1972. Monoclinic structure of synthetic $Ca_5(P\,O_4)_3$ Cl, chlorapatite. Acta Crystallographica B 28, 1840–1848.
Masciocchi, N., Artioli, G., 1996. Lattice parameters determination from powder diffraction data: results from a Round Robin project. Powder Diffraction 11, 253–258.
Matyi, R.J., Schwartz, L.H., Butt, J.B., 1987. Particle size, particle size distribution, and related measurements of supported metal catalysts. Catalysis Reviews 29 (1), 41–99.
McKinley, J.I., 1994. Bone fragment size in British cremation burials and its implications for pyre technology and ritual. Journal of Archaeological Science 21, 339–342.
Meneghini, C., Dalconi, M.C., Nuzzo, S., Mobilio, S., Wenk, R.H., 2003. Rietveld refinement on X-ray diffraction patterns of bioapatite in human fetal bones. Biophysical Journal 84 (3), 2021–2029.
Peterson, V.K., 2005. Lattice parameter measurement using Le Bail versus structural. Rietveld. refinement: a caution for complex, low symmetry systems. Powder Diffraction 20, 14–17.
Piga, G., Malgosa, A., Mazzarello, V., Bandiera, P., Melis, P., Enzo, S., 2007. Anthropological and physico-chemical investigation on the burnt remains of Tomb IX in the “Sa Figu” hypogeal necropolis (Sassari-italy)-Early Bronze Age. International Journal of Osteoarcheology 18, 167–177.
Piga, G., Malgosa, A., Thompson, T.J.U., Enzo, S., 2008. A new calibration of the XRD technique for the study of archaeological burnt remains. Journal of Archaeological Science 35, 2171–2178.
Piga, G., Santos-Cubedo, A., Moya Solà, S., Brunetti, A., Malgosa, A., Enzo, S., 2009a. An X-ray diffraction (XRD) and X-ray fluorescence (XRF) investigation in human and animal fossil bones from Holocene to Middle Triassic. Journal of Archaeological Science 36, 1857–1868.
Piga, G., Thompson, T.J.U., Malgosa, A., Enzo, S., 2009b. The potential of X-ray diffraction (XRD) in the analysis of burned remains from forensic contexts. Forensic Science International 54 (3), 534–539.
Piga, G., Guirguis, M., Bartoloni, P., Malgosa, A., Enzo, S., 2010a. A funerary rite study in the Phoenician-Punic Necropolis of Mount Sirai (Carbonia-Sardinia-Italy). International Journal of Osteoarchaeology 20, 144–157.
Piga, G., Hernández-Gasch, J.H., Malgosa, A., Ganadu, M.L., Enzo, S., 2010b. Cremation practices coexisting at the S'Illot des Porros Necropolis during the Second Iron Age in the Balearic Islands (Spain). Homo 61, 440–452.
Piga, G., Santos-Cubedo, A., Brunetti, A., Piccinini, M., Napolitano, E., Malgosa, A., Enzo, S., 2011. A multi-technique approach by XRD, XRF, FT-IR to characterize the diagenesis of dinosaur bones from Spain. Palaeogeography, Palaeoclimatology, Palaeoecology 310, 92–107.
Popa, N.C., 1998. The (hkl) Dependence of diffraction-line broadening caused by strain and size for all Laue groups in rietveld refinement. Journal of Applied Crystallography 31, 176–180.
Posner, A.S., Perloff, A., Diorio, A.F., 1958. Refinement of the hydroxyapatite structure. Acta Crystallographica 11, 308–309.
Rietveld, H.M., 1967. Line profiles of neutron powder-diffraction peaks for structure refinement. Acta Crystallographica 22, 151–152.
Shinomiya, T., Shinomiya, K., Orimoto, C., Minami, T., Tohno, Y., Yamada, M., 1998. In- and out-flows of elements in bones embedded in reference soils. Forensic Science International 98, 109–118.
Thompson, T.J.U., 2005. Heat-induced dimensional changes in bone and their consequences for forensic anthropology. Journal of Forensic Science 50 (5), 1008–1015.
Trujillo-Mederos, A., Alemán, I., Botella, M., Bosch, P., 2011. Changes in human bones boiled in seawater. Journal of Archaeological Science 39, 1072–1079.
Whyte, T., 2001. Distinguishing remains of human cremations from burned animal bones. Journal of Field Archaeology 28, 437–448.
Wopenka, B., Pasteris, J.D., 2005. A mineralogical perspective on the apatite in bone. Materials Science and Engineering C 25, 131–143.
Yashima, M., Yonehara, Y., Fujimori, H., 2011. Experimental visualization of chemical bonding and structural disorder in hydroxyapatite through charge and nuclear-density analysis. Journal of Physic Chemistry 115, 25077–25087.
Young, A., 1993. The Rietveld Method. IUCr, Oxford Science Publications.